Hindawi Publishing Corporation
Mobile Information Systems
Volume 2016, Article ID 8267407, 11 pages
http://dx.doi.org/10.1155/2016/8267407

Research Article

A Fast Self-Planning Approach for Fractional Uplink Power Control Parameters in LTE Networks

J. A. Fernández-Segovia,[1] S. Luna-Ramírez,[1] M. Toril,[1] and C. Úbeda[2]

[1]*Ingeniería de Comunicaciones, Universidad de Málaga, Campus de Teatinos S/N, 29071 Málaga, Spain*
[2]*Ericsson, Calle de la Retama 1, 28045 Madrid, Spain*

Correspondence should be addressed to J. A. Fernández-Segovia; jfs@ic.uma.es

Received 22 July 2016; Accepted 19 September 2016

Academic Editor: Jung-Ryun Lee

Uplink Power Control (ULPC) is a key feature of mobile networks. Particularly, in LTE, Physical Uplink Shared Channel (PUSCH) performance strongly depends on Uplink Power Control configuration. In this work, a methodology for the self-planning of uplink Fractional Power Control (FPC) settings is presented. Values for nominal power and channel path-loss compensation factor are proposed. The method is designed for the planning and operational (replanning) stages. A very fast solution for FPC setting can be achieved by the combination of several simple solutions obtained by assuming some simplifications. First, the FPC planning problem is formulated analytically on a cell basis through the combination of multiple regular scenarios built on a per-adjacency basis from a live scenario. Secondly, detailed inspection of the FPC parameter values aims to identify the most important variables in the scenario impacting optimal FPC settings. Finally, regression equations can be built based on those key variables for a simple FPC parameter calculation, so computational costs are extremely reduced. Results show that network performance with the proposed FPC parameter settings is good when compared with typical FPC configurations from operators.

1. Introduction

Mobile Communication Networks have experienced strong evolution in the last years. The development of new radio access technologies has increased network capacity and quality significantly, especially with the UMTS Long-Term Evolution (LTE) [1]. Simultaneously, the appearance of the so-called *smartphones* has changed the traffic behavior carried by mobile networks, where data transmission (and not voice calls) is the traffic benchmark, and, as a consequence, data transmission enhancement has been the main focus in present networks [2]. These factors have strengthened the role of network planning when there is a desire to improve overall network performance. Before the network deployment stage, network planning aims to get the best network performance in a concrete scenario. Trade-off between network capacity and coverage is the most limiting factor for network planning [3].

Regardless of the network radio access technology, proper network planning allows the operator to identify key network areas, which eases proper network dimensioning and enables the prediction of future bottlenecks. Thus, network planning is useful to avoid or, at least, delay subsequent capital investments [4, 5]. The growth of application data traffic has led to changes in network planning approaches trying to predict how the user experience is. Whereas former approaches have focused on network performance indicators, user-centric statistics are now the preference (e.g., average and cell-edge user throughput) [6].

Cellular network planning can be divided depending on the network system to be planned: core and Radio Access Network (RAN). While the core network planning relies mainly on dimensioning processes, RAN planning comprises radio dimensioning and radio parameter configuration [3, 7, 8]. Network operators do not usually take advantage of radio parameter configuration due to the inherent complexity of finding optimal parameter settings for every cell in the network. Thus, operators usually set radio parameters to some network-wide values recommended by vendors, which work reasonably well in most cases, but some additional network improvement is discarded. To revert this situation, the

3rd Generation Partnership Project (3GPP) has defined the requirements for the automation of planning, optimization, and self-healing in mobile networks [9]. As a result, network self-planning has been identified as an important process in Self-Organizing Networks (SON) now [5, 10, 11] and in the future [12].

Power Control (PC) is one of the most impacting algorithms in network performance. Fractional Power Control (FPC) has been selected for the Physical Uplink Shared Channel (PUSCH) in LTE [13, 14]. Consequently, FPC algorithm controls LTE uplink performance, which makes its configuration an ideal candidate for self-planning purposes. In fact, the variability of radio conditions such as propagation losses and interference level makes it difficult to set an optimal value for FPC parameters. For this reason, network operators use safe network-wide recommended values. As a consequence, suboptimal performance is achieved by the network. Hence, even if this can be solved in the operational stage, the provision of proper initial FPC settings would be valuable for network operators. Additionally, the research of low computational complexity methodologies for FPC self-planning is of high interest in the development of SON algorithms.

2. Related Work and Contribution

There is a wide background regarding FPC performance in LTE uplink. First, a performance analysis of open-loop FPC is presented in [15, 16], whereas closed-loop behavior was analyzed in [17–19]. Moreover, more sophisticated Power Control schemes for LTE were assessed in later studies [20, 21]. In those schemes, interference or load conditions were taken into consideration.

A sensitivity analysis of FPC parameters is performed in [22]. The analysis relies on system-level simulations and the results suggest a suboptimal parameter configuration for noise-limited and interference-limited scenarios. Obviously, the overall problem solution is not as simple, since it is a non-separable and nonlinear large-scale optimization problem. However, it is the start point in the search of more complex solutions. In [23], the FPC parameter settings problem in a single cell is formulated as a classical optimization problem, where average user throughput and cell throughput are taken as figures of merit for the optimization process. An extension of this analysis to a multicell scenario is done in [24] by formulating FPC as a noncooperative game model where a heuristic iterative optimization algorithm solves the problem. More conscientiously, a self-planning method for selecting the best parameter settings in FPC on a per-cell basis in an irregular LTE scenario is proposed in [25]. It is based on an exhaustive search approach using Taguchi's method over a system-level simulator. There are other studies considering tuning algorithms for the network operational stage. These self-tuning algorithms, which have been conceived for the operational stage, can also be applied in the planning stage, provided that a system model is available (e.g., a system-level simulator). For instance, a self-tuning algorithm is proposed in [26] to control interference by performing dynamical adjustment of nominal power parameter based on the overload indicator [27]. Likewise, a self-tuning algorithm for FPC is proposed in [28] based on fuzzy-reinforcement learning techniques. Most of these self-tuning algorithms need iterative evaluation of the system model for many different parameter settings, thus emulating the realistic network behavior. As a consequence, this iterative process is adequate for live networks, where performance measurements are provided. However, this is not the case of network planning, where computational cost increases with the complexity of the implemented system model. For this reason, most existing FPC planning methods rely on simple analytical models, which eases scalability and performance assessment.

A more computationally efficient planning method is presented in [29]. The method relies on an analytical model that predicts the influence of the nominal power and path-loss compensation factor on call acceptance probability for a previously defined spatial user distribution. A suboptimal solution for these parameters is computed by a local greedy search algorithm. In the same way, a computationally efficient method for self-planning Uplink Power Control parameters in LTE is presented in [30]. This method proposes a heuristic algorithm that can handle irregular scenarios at a low computational complexity. For this purpose, the parameter planning problem in a cell is formulated analytically through the combination of multiple regular scenarios built on a per-adjacency basis. However, in [30], Nonfractional Power Control is considered, assuming total propagation losses compensation.

To the authors' knowledge, few of the previous references handle irregular scenarios at a low computational cost and none of them propose some simple model with the aim of getting near-optimal FPC parameter values depending on scenario details.

In this paper, a fast method for the self-planning of FPC parameters in LTE uplink is proposed. The self-planning method determines the nominal PUSCH power, P_0, and the path-loss compensation, α, parameters in FPC. Similar to [30], to deal with scenario irregularities, the parameter setting problem is solved by the aggregation of multiple scenarios defined on a per-adjacency basis. Moreover, with the aim of minimizing computational complexity, solutions provided by the self-planning method are further analyzed and a simple model for the estimation of FPC parameter values is proposed.

Unlike [30], the decision variables in this work are P_0 and α, instead of P_0 and uplink cell load, U_{UL}. The approach in [30] is suitable for the planning stage, when performance measurements (PMs) are not available and the maximum cell loads are still design variables. However, it is limited to some first vendor releases, where α was a system constant ($\alpha = 1$). In contrast, the approach proposed here is conceived for the operational stage, when input parameters can be taken from network PMs. Thus, U_{UL} is an input parameter taken from statistics of Physical Resource Block (PRB) utilization ratio in the network management system. Likewise, FPC is considered here ($\alpha \leq 1$). Moreover, the optimization criterion is different from that used in [30].

The main contributions of this work are (a) a sensitivity analysis of FPC parameter solutions in a realistic network

implemented over a system-level simulator, (b) a thorough analysis of how FPC parameter values are related to LTE scenario characteristics and the identification of the most significant scenario parameters affecting FPC setting, and (c) a highly computationally efficient methodology to configure FPC parameters. The rest of the paper is organized as follows. In Section 3, the system model is outlined. The self-planning algorithm is presented in Section 4. Performance assessment is carried out in Section 5. Finally, concluding remarks are given in Section 6.

3. Fractional Power Control in LTE Uplink

Three physical channels are defined for LTE uplink: Physical Random Access Channel (PRACH), Physical Uplink Shared Channel (PUSCH), and Physical Uplink Control Channel (PUCCH) [31]. Attending to LTE standards, Uplink Power Control feature applies to PUSCH and PUCCH [14]. Specifically, PUSCH is used to transmit user data and control information for active users. Uplink Power Control (ULPC) behavior for PUSCH is defined as

$$P_{\text{tx}} = \min \left\{ P_{\text{tx}_{\text{max}}}, \underbrace{P_0 + \alpha \cdot \text{PL}}_{\substack{\text{basic open-loop} \\ \text{operating point}}} + \underbrace{\Delta_{\text{TF}} + f\left(\Delta_{\text{TPC}}\right)}_{\text{dynamic offset}} + \underbrace{10 \cdot \log_{10} M_{\text{PUSCH}}}_{\text{bandwidth factor}} \right\}, \tag{1}$$

where $P_{\text{tx}_{\text{max}}}$ is the maximum User Equipment (UE) transmit power, α is the channel path-loss compensation factor, PL are the propagation losses, M_{PUSCH} is the number of PRBs assigned to the UE, and $\Delta_{\text{TF}} + f(\Delta_{\text{TPC}})$ is a dynamic term that depends on the selected modulation scheme and power control commands sent by the eNodeB (eNB).

As shown in (1), transmit power depends on three terms: the basic open-loop operating point, dynamic offset which represents closed-loop corrections, and a multiplicative factor depending on the bandwidth. It must be noted that, in open-loop behavior, the parameter α ($\alpha \in \{0, 0.4, 0.5, 0.6, 0.7, 0.8, 0.9, 1\}$) represents the fraction of PL which are compensated by the UE to guarantee the nominal PUSCH power, P_0. Thus, when path-loss compensation factor is different from one, ULPC is known as Fractional Power Control (FPC).

In this work, the system model is the same as the one used in [30]; that is, uplink Signal over Interference and Noise Ratio (SINR) is based in the emulation of the uplink scheduler proposed there.

4. Self-Planning Algorithm

In this section, a self-planning methodology for FPC parameters, namely, P_0 and α, is described. General considerations regarding the algorithm are first explained in Section 4.1. The algorithm operation for regular scenarios is described in Section 4.2, and the algorithm extension for irregular scenario is performed in Section 4.3. Finally, a detailed analysis of FPC solutions is approached in Section 4.4, with the aim of building a multivariate linear regression model with the most significant scenario parameters.

4.1. General Consideration. Mobile network performance is usually experienced as a trade-off between coverage and capacity so both characteristics cannot be optimized separately. This trade-off is known as the Coverage and Capacity Optimization (CCO) SON use case defined by 3GPP in [32]. Network coverage and capacity are usually measured with cell-edge user and cell-average throughput statistics, respectively [6, 33].

Self-planning of FPC parameter is a particular way to approach the CCO problem. On the one hand, changing P_0 in a cell i impacts coverage and capacity of cell i and its surrounding neighbors. High P_0 values force the UEs connected to cell i to transmit with higher power, increasing interference in adjacent cells. However, received signal in cell i is higher, and, thus, SINR (and, as a consequence, cell throughput) is increased. Conversely, low P_0 values decrease transmit power for UEs in the cell, reducing interference in adjacent cells, which favors coverage of surrounding cells at the expense of reducing coverage and capacity of the considered cell. Regarding α parameter, different α settings impact similarly the UE transmit power, so it can be also used to manage interference between cells.

In any case, P_0 and α best settings are both very influenced by the particular topology and radio propagation conditions in the network scenario. This is especially important when irregular scenarios (which are majority) are considered. A cell-based FPC configuration can reach the best network performance by adapting P_0 and α settings to every cell environment. As a consequence, the resulting CCO problem is a nonseparable multivariable optimization problem in which all cells are jointly optimized. In other words, the solution space is $(N_{v_{P_0}} \cdot N_{v_\alpha})^{N_c}$, where $N_{v_{P_0}}$ and N_{v_α} are the number of possible values for P_0 and α parameters and N_c is the number of cells to be planned. The large size of the solution space prevents the use of exact algorithms, which are substituted by heuristic algorithms, for example, Taguchi's method [25], greedy search [29], or simulated annealing.

In this work, the methodology described in [30] is reproduced to reduce the algorithm search space. The global multivariate optimization problem is divided into N_c independent bivariate subproblems. The following subsections describe the optimization process in a regular scenario and then the extension to irregular scenarios and later an analysis of the algorithm solution that allows optimizing computational complexity by a regression model.

4.2. Regular Scenario. To design the self-planning algorithm, a sensitivity analysis of FPC parameters is carried out over a simple regular scenario. This regular scenario consists in seven trisectorial sites, specifically one central site surrounded by six adjacent sites, as shown in Figure 1. In such scenario, FPC parameters P_0 and α are configured uniformly in all cells. Then, parameters are separately swept

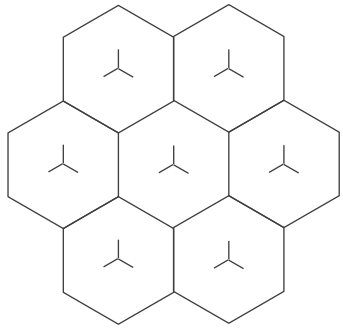

Figure 1: Regular scenario used in FPC parameter sensitivity analysis.

Table 1: Simulation parameters.

Parameters	Settings
Carrier bandwidth	10 MHz (50 PRBs)
Carrier frequency	2 GHz
Cell layout	7 eNBs, 21 sectors, regular grid (40 m resolution)
Distance attenuation	COST 231 [36]
Thermal noise density	−174 dBm/Hz
Cell radius	1.5 km (3 km intersite distance)
eNB antenna height	30 m
eNB antenna tilt	5°
eNB antenna pattern and gain	3GPP ideal [37]
Max. UE transmit power	23 dBm
Path-loss compensation factor, α	(0.4, 0.5, 0.6, 0.7, 0.8, 0.9, 1)
Cell load	100%
Traffic model	Full buffer

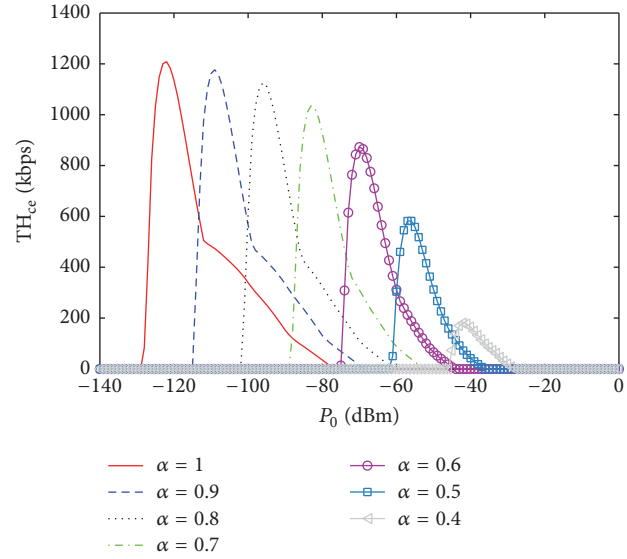

Figure 2: Cell-edge throughput performance in regular scenarios.

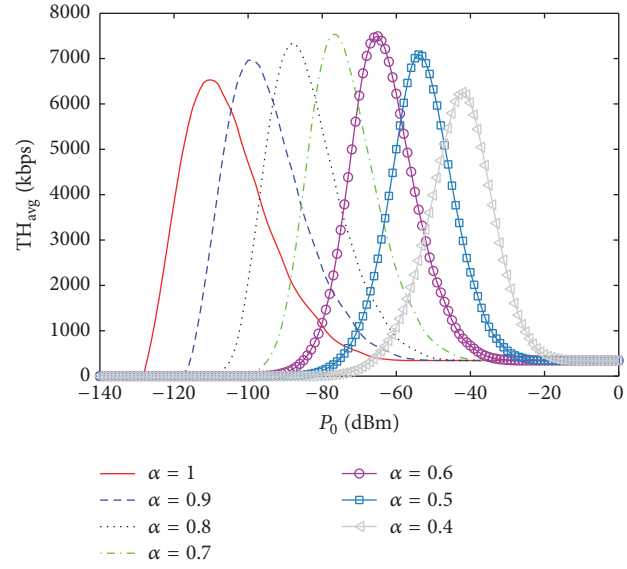

Figure 3: Cell-average user throughput performance in regular scenarios.

and coverage and capacity indicators are measured in one cell of the centre site. The rest of the simulation parameters are shown in Table 1.

Figures 2 and 3 show cell-edge and cell-average user throughput for cell i, $TH_{ce}(i)$ and $TH_{avg}(i)$, respectively, with different P_0 and α settings. Every curve in Figure 2 shows a similar behavior. With low P_0 values, increasing P_0 leads to an improvement in TH_{ce}. After that initial improvement, additional P_0 increases lead to TH_{ce} decreases due to intercell interference issues. Thus, an optimal P_0 value, $P_{0,opt}^{(ce)}$, can be defined (i.e., TH_{ce} is maximum for that $P_{0,opt}^{(ce)}$ value). A similar behavior is observed for TH_{avg} performance in Figure 3. Optimal P_0 has a different value when TH_{avg} performance is considered (i.e., $P_{0,opt}^{(ce)} \neq P_{0,opt}^{(avg)}$). On the other hand, decreasing α has a high impact on coverage and capacity figures. Maximum TH_{ce} value decreases with α due to uncompensated losses, whereas maximum TH_{avg} value increases due to the interference decreases for lower α values. Moreover, curves in Figures 2 and 3 are displaced to the right due to path-loss compensation impact over UE transmit power in (1). Additionally, the difference between optimal P_0 values, $P_{0,opt}^{(avg)}$-$P_{0,opt}^{(ce)}$, is decreased for lower α values (and, thus, the best coverage and capacity performance could be reached simultaneously).

Based on the behavior observed in Figures 2 and 3, a self-planning algorithm for P_0 and α parameters in a regular scenario is designed. The proposed algorithm finds the optimal P_0 and α settings by a simple gradient search

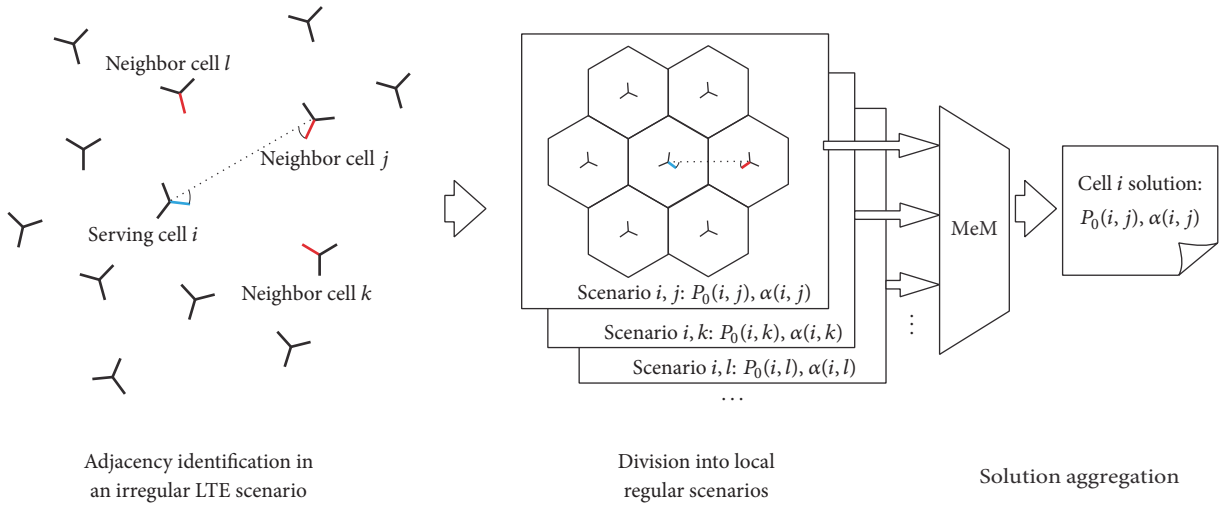

Figure 4: Optimization process for irregular scenarios.

which maximizes TH_{ce} and TH_{avg} according to a *trade-off* value, t, as

$$\max_{(P_0,\alpha)} \left\{ t \cdot \mathrm{TH}_{ce}(i) + (1-t) \cdot \mathrm{TH}_{avg}(i) \right\}, \quad t \in [0,1]. \tag{2}$$

Note that in regular scenarios all cells are identically configured (i.e., $P_0(i) = P_0(j)$ and $\alpha(i) = \alpha(j), \forall i, j$).

4.3. Irregular Scenario. The previous section proposed a method for finding an optimal solution for FPC parameter settings in a regular scenario. However, mobile networks operate in realistic scenarios (where cells are not regular) with very different user and radio conditions along cells. Additionally, cell performance is also affected by the also irregular adjacent cells. Hence, these irregularities have to be considered to plan FPC parameters. In this work, irregularities are approached similarly to the algorithm presented in [30]. Figure 4 depicts this process in three different stages.

In the first stage, *the identification of adjacent cells in an irregular LTE scenario* is performed. To identify the most relevant adjacent cells for cell i, $N_{adj}(i)$, neighbors are sorted following the indicator NR_{UL}, defined as

$$\mathrm{NR}_{UL}(i,j) = L(i,j) - A_H(i,j) - A_V(i,j), \tag{3}$$

where $L(i, j)$ is the path-loss between the cell under study i and cell j and $A_h(i, j)$ and $A_v(i, j)$ are the horizontal and vertical gains for the antenna of cell i to the location of eNB j. First $N_{adj}(i)$ cells in the list are selected as adjacent cells.

In the second stage, *division into several local regular scenarios* is done. One regular scenario is built per serving cell i and neighbor cell j, based on the relative geometry between both cells. Relative antenna angles, antenna tilt, and height of both cells are kept from the irregular scenario. To compute interference levels in each regular scenario, it is assumed that all cells have the same uplink cell load, equal to that of the serving cell, $U_{UL}(i)$. Recall that $U_{UL}(i)$ is an input parameter taken from network measurements. Then, neighbor cell is replicated to complete the first tier of adjacent cells resulting in a regular scenario as that shown in Figure 1. $N_{adj}(i)$ regular scenarios are built per cell. Equation (2) is solved to find optimal P_0 and α for each scenario. Note that every regular scenario has different network parameters and has to be simulated (and solved) separately. At the end of this process, there are $N_{adj}(i)$ solutions (i.e., $P_0(i, j)$ and $\alpha(i, j)$ value for every j cell being adjacent to cell i), so some final criteria must be defined to obtain the final $P_0(i)$ and $\alpha(i)$ values.

Finally, in the third stage, the *aggregation of solutions* obtained from every regular scenario is carried out. As a result, a unique solution of the pair of parameters $P_0(i)$ and $\alpha(i)$ is given for each cell i. Different aggregation methods were tested in [30], although the so-called Medium Method (MeM) achieved better trade-off results. MeM calculates $P_0(i)$ and $\alpha(i)$ as the average value of all $P_0(i, j)$ and $\alpha(i, j)$ solutions. Hence, MeM is selected as the aggregation method in this work.

4.4. Regression Model for FPC Solutions. A self-planning algorithm for FPC parameters has been presented in previous sections. The proposed algorithm reduces the complexity of exhaustive search by breaking down the problem into many regular scenarios. Nonetheless, each of these regular scenarios has still to be simulated and solved. Thus, the computational complexity of the method can be reduced by deriving a simple analytical formula giving the optimal value of FPC parameters in terms of network parameters obtained from simulations. In this section, a thorough analysis of FPC optimal settings in a regular scenario is performed by means of multivariate linear regression (MLR) model inspection. The aim is to identify which are the most relevant variables in the scenario when finding optimal P_0 and α settings in

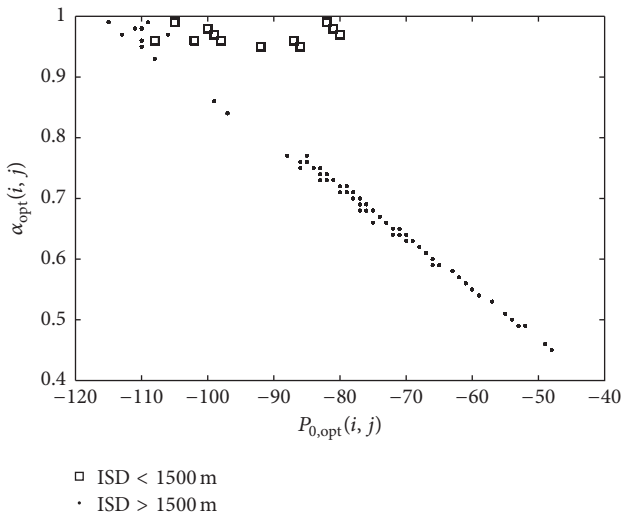

Figure 5: $P_{0,opt}(i, j)$ and $\alpha_{opt}(i, j)$ values.

a regular scenario. Thus, a set of regression equations for calculating optimal FPC settings is obtained as follows:

$$P_{0,opt}(c) = \beta_0 + \sum_{l=1}^{k} \beta_l \cdot p_l(c) + \epsilon,$$
$$\alpha_{opt}(c) = \beta_0 + \sum_{l=1}^{k} \beta_l \cdot p_l(c) + \epsilon, \quad (4)$$

where $P_{0,opt}(c)$ and $\alpha_{opt}(c)$ are the optimal solutions obtained from the self-planning approach for a combination c of independent variables (i.e., scenario configuration), l is used to index variables, p_l are the variables selected as candidate independent variables, β_l is the regression coefficient for each p_l, k is the number of candidate independent variables in the MLR model, and ϵ is the error term.

The first set of scenario variables to be considered in the regression analysis is as follows: (a) intersite distance, ISD, in a logarithmic scale as an indicator of propagation losses, (b) antenna height, h_b, in meters, (c) uplink cell load ratio, U_{UL}, (d) vertical antenna gain, V_G, measured in dB, as an indicator of the antenna tilt, and (e) horizontal gain, H_G, measured in dB, as an indicator of the relative angle between cells. A wide set of regular scenarios are built for different values of these variables. Specifically, 145800 different combinations of the independent variables have been tested. Note that a regular scenario can be built with a different value of the same variable for the central and surrounding cell (e.g., $h_b(i) \neq h_b(j)$ in a regular scenario). MLR model defined in (4) is, thus, built from $P_{0,opt}$ and α_{opt} solutions extracted from all the regular scenarios built according to the values set for these variables. MLR analysis has been performed for a fixed value of trade-off, $t = 0.5$.

A previous analysis of $P_{0,opt}$ and α_{opt} values obtained from the different regular scenarios is shown in Figure 5. Solutions in the figure are divided by ISD in the scenario. It is shown that there is a clear trend of optimal solutions with ISD. Parameter α_{opt} remains almost constant when ISD < 1500 m, whereas $P_{0,opt}$ moves in a wide range (20 dB). When ISD > 1500 m, the solution behavior is not constant, but lineal dependence between $P_{0,opt}$ and α_{opt} is shown. Thus, MLR model construction is performed in two stages: (a) small-medium cells (ISD < 1500 m) and (b) medium-large cells (ISD > 1500 m).

Table 2: MLR model for small-medium cells.

Regression statistics, ISD < 1500 m		
Determination coefficient	$R^{2(P_{0,opt})} = 0.9$	
	$P_{0,opt}$	
MLR analysis	$\widehat{\beta}_i$	P
Constant (β_0)	71.23	0
ISD [dB]	−5.437	0
$h_b(i)$ [m]	$-3.8E-15$	1
$h_b(j)$ [m]	$-2.24E-15$	1
$V_G(i)$ [dB]	$-2.22E-15$	1
$V_G(j)$ [dB]	0.372	0
U_{UL}	−0.05	0.471
H_G [dB]	−2.83	$1.5E-97$

4.4.1. Small-Medium Cells MLR Analysis. Table 2 details MLR model analysis when ISD < 1500 m. Subscript i in the table refers to the value of such parameter for the central cell in the regular scenario (e.g., antenna height in cell i), and j subscript refers to the neighbor cell (e.g., antenna height for neighbor cell j). As shown in the table, $P_{0,opt}$ is accurately predicted when all variables are considered ($R^2 = 0.9$). As seen in Figure 5, α_{opt} remains almost constant (between 0.95 and 1), so no MLR model is built and $\alpha_{opt} = 1$ is considered.

Attending to the p values in Table 2, ISD and $V_G(j)$ prove to be the most important variables when calculating $P_{0,opt}$. With a similar methodology to that described in [34], a simplified MLR model is constructed by following a variable elimination process. Initially, all variables in Table 2 are included in the model. Then, in each iteration, the least important variable (that with the highest p value) is eliminated until the determination coefficient, R^2, remains at an acceptable level (i.e., when the determination coefficient, R^2, is less than 0.7). The resulting model is

$$\widehat{P_{0,opt}} = 64.545 - 5.437 \cdot \text{ISD} + 0.372 \cdot V_G(j),$$
$$\widehat{\alpha_{opt}} = 1, \quad (5)$$

where $V_G(j)$ refers to the vertical gain of the neighbor cell j towards the cell under study. This simplified model reaches $R^2 = 0.894$.

4.4.2. Medium-Large Cells MLR Analysis. Analogously, Table 3 shows the MLR model with all variables when ISD > 1500 m. As shown in the table, $P_{0,opt}$ and α_{opt} can be determined with relatively good accuracy attending to the determination coefficient ($R^2 > 0.75$ in both cases).

Regarding the p values in Table 3, ISD, $V_G(j)$, and $U_{UL}(i)$ prove to be the most important variables when calculating

Table 3: MLR analysis for medium-large cells.

Regression statistics, ISD > 1500 m				
Determination coefficient	$R^{2(P_{0,\text{opt}})} = 0.76$		$R^{2(\alpha_{\text{opt}})} = 0.75$	
	$P_{0,\text{opt}}$		α_{opt}	
MLR analysis	$\widehat{\beta}_i$	P	$\widehat{\beta}_i$	P
Constant (β_0)	−423.53	0	3.639	0
ISD [dB]	10.527	0	−0.0893	0
$h_b(i)$ [m]	$-1.47E-15$	1	$2.91E-17$	1
$h_b(j)$ [m]	$-6.4E-16$	1	$2.03E-17$	1
$V_G(i)$ [dB]	$-3.29E-15$	1	$2.53E-17$	1
$V_G(j)$ [dB]	−0.258	$1.09E-296$	$2.44E-3$	0
U_{UL}	−17.083	0	0.144	0
H_G [dB]	−0.139	$1.3E-4$	$9.16E-4$	$3.08E-3$

$P_{0,\text{opt}}$ and α_{opt}. Again, a simplified MLR model is constructed and defined as

$$\begin{aligned}\widehat{P_{0,\text{opt}}} &= -425.73 + 10.53 \cdot \text{ISD} - 0.258 \cdot V_G(j) - 17.08 \\ &\quad \cdot U_{\text{UL}}(i), \\ \widehat{\alpha_{0,\text{opt}}} &= 3.65 - 0.0893 \cdot \text{ISD} + 0.00244 \cdot V_G(j) + 0.144 \\ &\quad \cdot U_{\text{UL}}(i).\end{aligned} \tag{6}$$

5. Performance Analysis

Solutions for FPC settings proposed by the algorithm presented in this work are assessed in a system-level simulator implementing a realistic scenario. The simulator is the same as the one used in [30]. For the sake of clarity, the different tests are described first in Section 5.1 and the results are commented on in Section 5.2. Additionally, some comments on time complexity are presented in Section 5.3.

5.1. Analysis Setup. A static system-level LTE simulator like that in [30, 35] is used. In the simulator, the analyzed area is divided into a regular grid of points, representing potential user locations. For each network parameter setting (i.e., a FPC parameter plan), the received signal level at each base station from each point is computed by a macrocellular propagation model including log-normal slow fading (no fast fading is considered). Then, the serving cell for each point is defined as that providing the maximum signal level. Interference level is estimated by considering a nonuniform spatial user and cell load distribution following a realistic pattern extracted from a live LTE network. Then, radio link quality and efficiency are computed. Finally, different PMs are calculated by aggregating the previous measurements across all points in the scenario. Only uplink is considered here.

Despite its simplicity, the simulator is designed to make the most of available network statistics to model a live macrocellular scenario. For this purpose, the simulator includes the following features:

(i) Delimitation of forbidden areas (i.e., points where users cannot be located) due to water resources by coastline files in Keyhole Markup Language (KML) format

(ii) Parameterization of antenna model on a cell basis (maximum gain, horizontal/vertical beamwidth, etc.) depending on vendor equipment

(iii) Initialization of cell load distribution across the scenario with uplink utilization ratio (U_{UL}) derived from counters in the network management system of a live LTE network

(iv) Adjustment of spatial user distribution within a cell on a distance ring basis from timing advance (TA) distributions

(v) Tuning of propagation model parameters based on the histogram of Reference Signal Received Power (RSRP) measurements

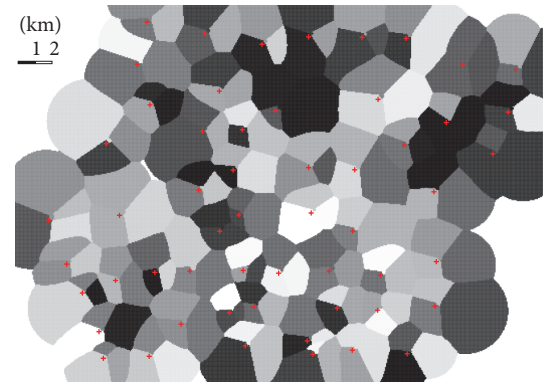

Figure 6: Simulated LTE network.

A live scenario is simulated. The scenario consists of 129 LTE cells covering a wide metropolitan area. Cells location, azimuth, antenna tilts, and uplink cell load are retrieved from network configuration management data stored in the operator network management system (NMS). In Figure 6, cell locations and services areas are represented.

Main configuration parameters of the simulated scenario are shown in Table 4. The rest of the simulation parameters were previously shown in Table 1.

Table 4: Network parameters.

Parameters	Settings
Carrier bandwidth	10 MHz (50 PRBs)
Carrier frequency	2.1 GHz
Cell layout	44 eNBs (129 sectors)
Intersite distance	0.45–4.5 km
eNB antenna height	15–54 m
eNB antenna tilt	0°–13°
Uplink cell load	5–19.2%

Three FPC parameter plans have been obtained under different trade-off conditions. FPC plans are calculated for $t = 0$ (a *capacity* oriented plan), $t = 1$ (a *coverage* oriented plan), and $t = 0.5$ (a *balanced* trade-off of capacity-coverage). Note that a FPC plan comprises $P_{0,\text{opt}}(i)$ and $\alpha_{\text{opt}}(i)$ values for every cell i in the scenario. As a benchmark for the solution comparison, different uniform FPC parameter settings (i.e., the same P_0 and α value for all cells) have also been simulated.

On the other hand and regarding the grade of complexity for simulations, three simulation configuration degrees are executed in ascending order of realism. In the lowest step, the simulator does not consider path-loss shadowing and uniform user spatial distribution is applied. In the second step, the simulator considers path-loss shadowing ($\sigma = 8$ dB) but still uses uniform user spatial distribution. Finally, in the third step, both path-loss shadowing and nonuniform user spatial distribution are considered. Here, it is worth noting that user spatial configurations are obtained from network realistic measurement.

To quantify solution performance, user-centric measurements are used. Overall cell-average user throughput, $\overline{\text{TH}_{\text{avg}}(i)}$, as the average of $\text{TH}_{\text{avg}}(i)$ for all cells in the scenario, is taken as a capacity indicator. Similarly, overall cell-edge user throughput, $\overline{\text{TH}_{\text{ce}}(i)}$, as the average of $\text{TH}_{\text{ce}}(i)$ for all cells in the scenario, is taken as a coverage indicator.

5.2. Results. Results are analyzed by simulator complexity and capacity/coverage trade-off first. Then, some comments on the performance of uniform parameter settings and time complexity are given.

5.2.1. Simulation Results with No Shadowing and Uniform Spatial User Distribution. Figure 7 shows the performance of the uniform FPC plans and trade-offs when no shadowing and uniform user distribution are considered. This figure can be considered as a *basic* case. Note that every plan is a point in the figure.

In the case of the capacity trade-off approach ($t = 0$), the proposed solution capacity ($\overline{\text{TH}_{\text{avg}}(i)}^{(\text{cap})} = 18180$ kbps) slightly outperforms the maximum capacity achieved by any uniform FPC parameter settings. However, coverage ($\overline{\text{TH}_{\text{ce}}(i)}^{(\text{cap})} = 8951$ kbps) is decreased by 7% with respect to the maximum coverage achieved by benchmark curves.

For the balanced trade-off approach ($t = 0.5$), coverage indicator ($\overline{\text{TH}_{\text{ce}}(i)}^{(\text{bal})} = 10030$ kbps) outperforms the best coverage obtained by benchmark curves by 4%, but capacity decreases by 5.7% in comparison with the capacity approach. This is due to the trade-off between capacity and coverage.

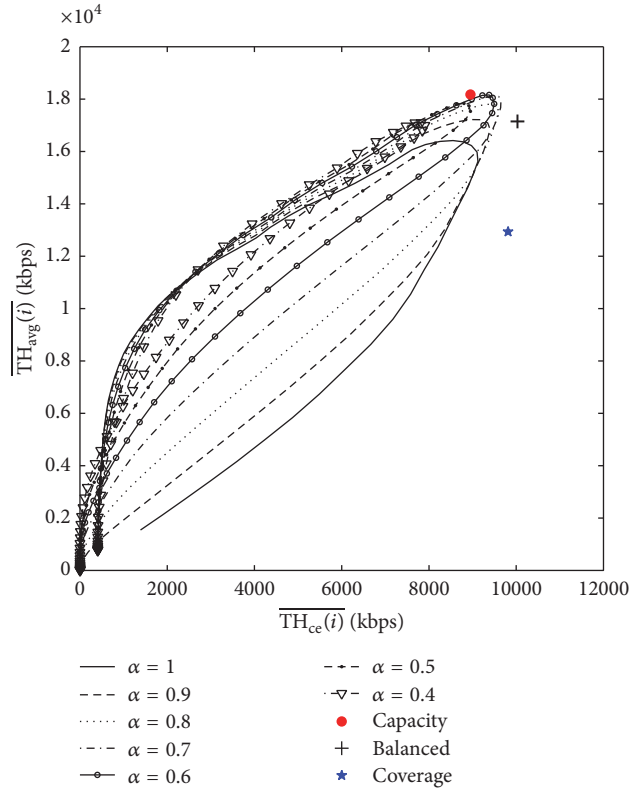

Figure 7: Simulation results, no shadowing, uniform traffic distribution.

Similar to the balanced trade-off approach, in the coverage approach ($t = 1$), coverage ($\overline{\text{TH}_{\text{ce}}(i)}^{(\text{cov})} = 9816$ kbps) outperforms the best coverage obtained by any uniform FPC plan. Nonetheless, capacity is highly degraded (downgrade of 29% compared to capacity approach) as better coverage is obtained at low P_0 values, where the distance between optimal P_0 for capacity and coverage is higher as explained in Section 4.2.

As expected, balanced trade-off approach outperforms all other approaches, because it considers both capacity and coverage indicators for the construction of FPC plan.

5.2.2. Simulation Results with Shadowing and Uniform Spatial User Distribution. Figure 8 shows similar information when shadowing is included. The overall behavior is the same as that behavior shown in the basic case, Figure 7, but coverage values have decreased in all cases due to the inclusion of path-loss shadowing feature.

For the capacity approach, $\overline{\text{TH}_{\text{avg}}(i)}^{(\text{cap})} = 17800$ kbps, performing as good as the best uniform plan. However, $\overline{\text{TH}_{\text{ce}}(i)}^{(\text{cap})} = 5729$ kbps, which is 25% lower than the best performance achieved by benchmark curves ($\overline{\text{TH}_{\text{ce}}(i)}^{(\text{max})} = 7652$ kbps).

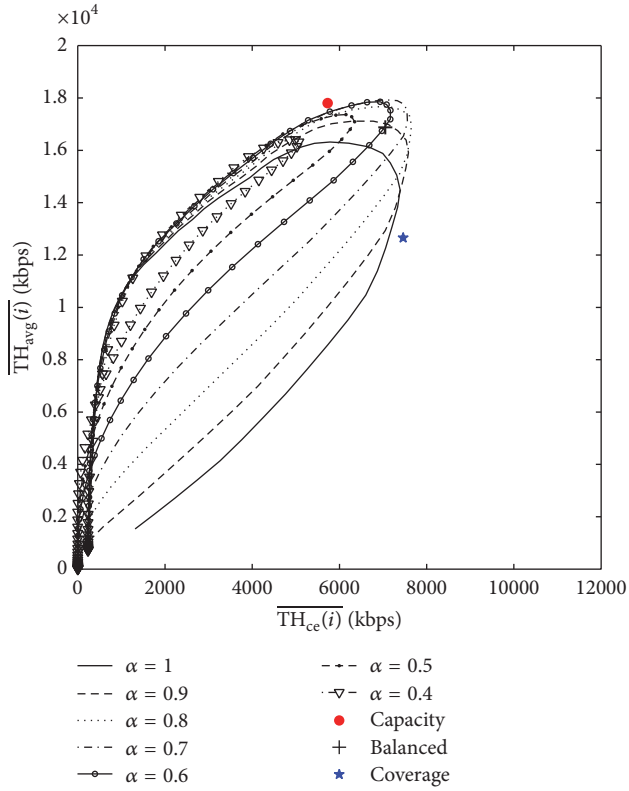

FIGURE 8: Simulation results with shadowing, uniform traffic distribution.

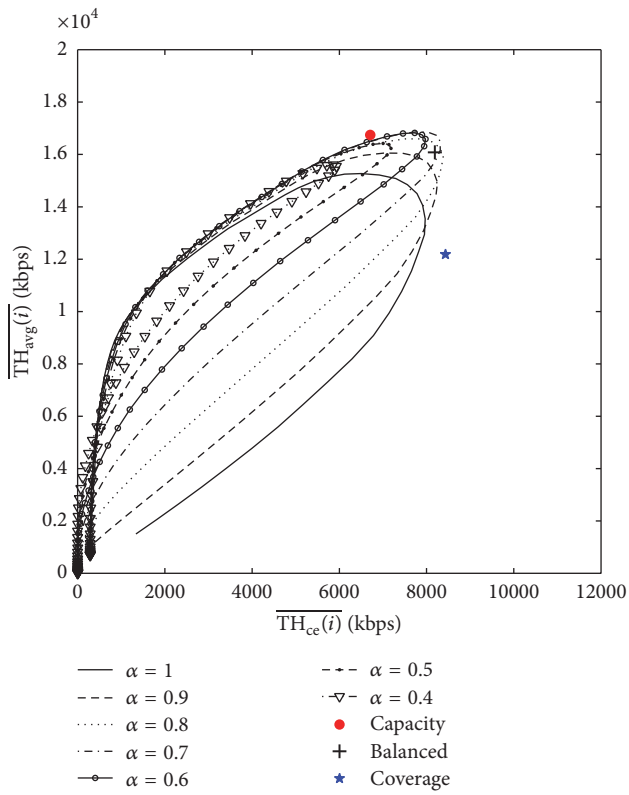

FIGURE 9: Simulation results with shadowing and nonuniform traffic distribution.

When the balanced trade-off is considered, both coverage and capacity are degraded. Thus, capacity and coverage indicators are, respectively, 5.2% and 7.9% below the maximum achieved by other methods.

Coverage approach reaches $\overline{TH_{ce}(i)}^{(cov)} = 7461$ kbps, degrading only by 2.5% compared to the maximum achieved by other methods. However, capacity indicator ($\overline{TH_{avg}(i)}^{(cov)} = 12650$ kbps) is degraded by 29.2% regarding the maximum achieved by the capacity approach.

In this case, balanced trade-off approach is again the best solution proposed by the method. However, capacity and coverage values are below the maximum achieved by the set of uniform configurations. Nonetheless, the performance degradation remains below 8%.

5.2.3. Simulation Results with Shadowing and Nonuniform Spatial User Distribution. Finally, Figure 9 shows performance results including shadowing and nonuniform user distribution. Again, a similar behavior is observed, but some additional comments must be highlighted.

About the performance of capacity approach, capacity indicator ($\overline{TH_{avg}(i)}^{(cap)} = 16750$ kbps) is slightly degraded (0.71%) compared to the maximum achieved by all other solutions. Nonetheless, the coverage indicator ($\overline{TH_{ce}(i)}^{(cap)} = 6708$ kbps) is 19.33% below the maximum obtained by any uniform FPC plan. The balanced trade-off approach experiences a reduction of 4.7% and 1.57% for capacity and coverage indicators, respectively, compared to the other approaches. Regarding coverage approach, coverage indicator ($\overline{TH_{ce}(i)}^{(cov)} = 8435$ kbps) slightly outperforms (1.43%) the best result achieved by any other solution. Nonetheless, capacity indicator is degraded by 27.8% when compared to the best capacity performance for any other FPC plan.

Note that Figure 9 reflects the most realistic situation. Hence, performance results from the proposed FPC plans (i.e., capacity, coverage, and balanced approaches) perform similarly to the best uniform FPC plans. However, execution time when getting FPC plans with the proposed methodology is extremely decreased.

5.2.4. Uniform Parameter Settings. Figures 7, 8, and 9 show the performance for different network-wide uniform FPC settings. The impact of P_0 changes on capacity and coverage performance is the same as described in [30], and, hence, it is not detailed in this work. However, some comments on LTE network capacity and coverage regarding uniform α settings are outlined.

The different curves in those figures correspond to different α values. As expected by the analysis carried out in Section 4.2, maximum capacity is not achieved for total compensation, $\alpha = 1$. On the contrary, maximum capacity is achieved for medium α values (0.7–0.8). Regarding coverage and similar to capacity, there is a trade-off in the best value of α for coverage. Another interesting behavior is observed when α decreases. In this situation, curves are narrower. Higher and lower P_0 configurations have a similar impact on

capacity and coverage performance. This effect is produced by the decrement in $P_{0,\text{opt}}^{(\text{avg})}$-$P_{0,\text{opt}}^{(\text{ce})}$ when decreasing α described in Section 4.2.

5.3. Execution Time. All tests have been run on an Intel® Xeon© machine at 3.47 GHz with 12 GB of RAM. The execution time required to build curves from uniform FPC plans (i.e., uniform P_0 and α settings) was 974.67 seconds on average. The self-planning method proposed in this work for calculating cell-individual FPC parameters took an average of 64.5 seconds (0.5 seconds per cell), which is a gain of 15 times. However, if MLR models are used, execution time is almost instantaneous, which is quite useful in self-planning tools.

It is also worth mentioning that a uniform FPC requires resimulation of the whole scenario when a new cell is added to an existing (i.e., already planned) scenario. On the contrary, the self-planning method proposed in this work only needs to solve $1 + N_{\text{neigh}}(i)$ subproblems.

6. Conclusion

In this work, a very fast approach for the self-planning of FPC parameters in LTE uplink has been proposed. The method deals with irregular scenarios by dividing the large-scale multivariable optimization problem into multiple simple optimization problems, where a regular scenario is assumed on a per-adjacency basis. In those simplified scenarios, optimal FPC settings are calculated by an exhaustive search method. Additionally, optimal solutions have been analyzed and a set of regression equations have been given for the estimation of optimal FPC settings and, hence, reducing complexity and time execution. Finally, per-adjacency solutions are aggregated by averaging them into one solution per cell in the scenario. As a consequence, the proposed methodology is able to cope with complex irregular scenarios at a very low computational cost, which is very useful for self-planning tools. Performance assessment has been carried out over a system-level simulator implementing a real scenario. Results show that the proposed solutions work reasonably well when compared with uniform FPC plans designed by an exhaustive search process. Capacity performance is degraded by 4.7% and coverage performance by 1.57%. The main gain is in the execution time, which allows this approach to be used in frameworks where fast planning is required at a very low computational cost.

The proposed FPC self-planning methodology can be implemented as part of a centralized SON service. The system would retrieve eNB needed information from the NMS (location, azimuth, antenna tilt, uplink cell load, etc.). On the one hand, the method would perform self-configuration of every eNB in the network in the deployment stage. On the other hand, the method would reconfigure FPC parameter settings when a new eNB is added/removed from the network during the operational stage.

Competing Interests

The authors declare that they have no competing interests.

Acknowledgments

This work has been funded by the Spanish Ministry of Economy and Competitiveness (TEC2015-69982-R), Optimi-Ericsson and Agencia IDEA (Consejería de Ciencia, Innovación y Empresa, Junta de Andalucía, Ref. 59288), and FEDER.

References

[1] 3GPP TS 36.301, LTE; Evolved Universal Terrestrial Radio Access (E-UTRA); Long Term Evolution (LTE) Physical Layer; General Description. V8.3, April 2009.

[2] NSN: Understanding Smartphone Behavior in the Network, Nokia Solutions and Networks Smart Labs, white paper, 2013.

[3] A. R. Mishra, *Advanced Cellular Network Planning and Optimisation*, John Wiley & Sons, New York, NY, USA, 2006.

[4] A. Hoikkanen, "Economics of 3G long-term evolution: the business case for the mobile operator," in *Proceedings of the 4th IEEE and IFIP International Conference on Wireless and Optical Communications Networks (WOCN '07)*, pp. 1–5, July 2007.

[5] S. Hamalainen, H. Sanneck, and C. Sartori, *LTE Self-Organising Networks (SON)*, John Wiley & Sons, New York, NY, USA, 2011.

[6] P. Oliver-Balsalobre, M. Toril, S. Luna-Ramírez, and J. M. Ruiz Avilés, "Self-tuning of scheduling parameters for balancing the quality of experience among services in LTE," *EURASIP Journal on Wireless Communications and Networking*, vol. 2016, no. 1, pp. 1–12, 2016.

[7] J. Lempiainen and M. Manninen, *Radio Interface System Planning for GSM/GPRS/UMTS*, Springer, New York, NY, USA, 2001.

[8] J. Laiho, A. Wacker, and T. Novosad, *Radio Network Planning and Optimisation for UMTS*, John Wiley & Sons, New York, NY, USA, 2002.

[9] 3GPP, "Telecommunication management; self-organizing networks (SON); concepts and requirements. V9," 3GPP TS 32.500, 2009.

[10] NGMN Use Cases Related to Self Organising Network, Overall Description, http://www.ngmn.org.

[11] J. Ramiro and K. Hamied, *Self-Organizing Networks: Self-Planning, Self-Optimization and Self-Healing for GSM, UMTS and LTE*, John Wiley & Sons, New York, NY, USA, 2011.

[12] L. Jorguseski, A. Pais, F. Gunnarsson, A. Centonza, and C. Willcock, "Self-organizing networks in 3GPP: standardization and future trends," *IEEE Communications Magazine*, vol. 52, no. 12, pp. 28–34, 2014.

[13] J. F. Whitehead, "Signal-level-based dynamic power control for co-channel interference management," in *Proceedings of the 43rd IEEE Vehicular Technology Conference (VTC '93)*, pp. 499–502, May 1993.

[14] 3GPP TS 36.213, Physical Layer Procedures, V8.6, September 2009.

[15] W. Xiao, R. Ratasuk, A. Ghosh, R. Love, Y. Sun, and R. Nory, "Uplink power control, interference coordination and resource allocation for 3GPP E-UTRA," in *Proceedings of the IEEE 64th Vehicular Technology Conference (VTC '06)*, pp. 1–5, IEEE, Montreal, Canada, September 2006.

[16] A. M. Rao, "Reverse link power control for managing inter-cell interference in orthogonal multiple access systems," in *Proceedings of the IEEE 66th Vehicular Technology Conference (VTC-Fall '07)*, pp. 1837–1841, Baltimore, Md, USA, September 2007.

[17] A. Simonsson and A. Furuskär, "Uplink power control in LTE—overview and performance: principles and benefits of utilizing rather than compensating for SINR variations," in *Proceedings of the 68th Semi-Annual IEEE Vehicular Technology (VTC '08)*, pp. 1–5, September 2008.

[18] B. Muhammad and A. Mohammed, "Performance evaluation of uplink closed loop power control for LTE system," in *Proceedings of the IEEE 70th Vehicular Technology Conference Fall (VTC '09)*, pp. 1–5, Anchorage, Alaska, USA, September 2009.

[19] B. Muhammad and A. Mohammed, "Uplink closed loop power control for LTE system," in *Proceedings of the 6th International Conference on Emerging Technologies (ICET '10)*, pp. 88–93, IEEE, Islamabad, Pakistan, October 2010.

[20] S. Yang, Q. Cui, X. Huang, and X. Tao, "An effective uplink power control scheme in CoMP systems," in *Proceedings of the IEEE 72nd Vehicular Technology Conference Fall (VTC-Fall '10)*, pp. 1–5, Ottawa, Canada, September 2010.

[21] N. J. Quintero, *Advanced power control for UTRAN LTE uplink [Ph.D. thesis]*, Department of Electronic Systems, Aalborg University, 2008.

[22] C. Ú. Castellanos, D. L. Villa, C. Rosa et al., "Performance of uplink fractional power control in UTRAN LTE," in *Proceedings of the IEEE 67th Vehicular Technology Conference (VTC '08)*, pp. 2517–2521, IEEE, Singapore, May 2008.

[23] C. Suh, A. T. Koc, and S. Talwar, "Tradeoff power control for cellular systems," in *Proceedings of the IEEE Global Telecommunications Conference (GLOBECOM '09)*, pp. 1–6, Honolulu, Hawaii, USA, December 2009.

[24] S. Xu, M. Hou, K. Niu, Z.-Q. He, and W.-L. Wu, "Coverage and capacity optimization in LTE network based on non-cooperative games," *The Journal of China Universities of Posts and Telecommunications*, vol. 19, no. 4, pp. 14–42, 2012.

[25] A. Awada, B. Wegmann, I. Viering, and A. Klein, "Optimizing the radio network parameters of the long term evolution system using Taguchi's method," *IEEE Transactions on Vehicular Technology*, vol. 60, no. 8, pp. 3825–3839, 2011.

[26] C. Ú. Castellanos, F. D. Calabrese, K. I. Pedersen, and C. Rosa, "Uplink interference control in UTRAN LTE based on the overload indicator," in *Proceedings of the IEEE 68th Vehicular Technology Conference (VTC '08)*, pp. 1–5, IEEE, Calgary, Canada, September 2008.

[27] 3GPP, "Overload indicator handling for LTE, TSG RAN WG1 #50bis Meeting. V8.6," 3GPP R1-074349, ETSI, Sophia Antipolis Cedex, France, 2007.

[28] M. Dirani and Z. Altman, "Self-organizing networks in next generation radio access networks: application to fractional power control," *Computer Networks*, vol. 55, no. 2, pp. 431–438, 2011.

[29] K. Majewski and M. Koonert, "Analytic uplink cell load approximation for planning fractional power control in LTE networks," *Telecommunication Systems*, vol. 52, no. 2, pp. 1081–1090, 2013.

[30] J. Á. Fernández-Segovia, S. Luna-Ramírez, M. Toril, A. B. Vallejo-Mora, and C. Úbeda, "A computationally efficient method for self-planning uplink power control parameters in LTE," *EURASIP Journal on Wireless Communications and Networking*, vol. 2015, no. 1, article 80, 2015.

[31] 3GPP TS 36.211, LTE; Evolved Universal Terrestrial Radio Access (E-UTRA); Physical Channels and Modulation. V12.3, Octubre 2014.

[32] 3GPP TS 32.521, Technical Specification Group Services and System Aspects; Telecommunications Management; Self-Organizing Networks (SON) Policy Network Resource Model (NRM) Integration Reference Point (IRP); Requirements. V9, March 2010.

[33] P. Patras, A. Banchs, and P. Serrano, "A control theoretic approach for throughput optimization in IEEE 802.11e EDCA WLANs," *Mobile Networks and Applications*, vol. 14, no. 6, pp. 697–708, 2009.

[34] J. A. Fernández-Segovia, S. Luna-Ramírez, M. Toril, and J. J. Sánchez-Sánchez, "Estimating cell capacity from network measurements in a multi-service LTE system," *IEEE Communications Letters*, vol. 19, no. 3, pp. 431–434, 2015.

[35] V. Buenestado, M. Toril, S. Luna-Ramirez, J. M. Ruiz-Aviles, and A. Mendo, "Self-tuning of remote electrical tilts based on call traces for coverage and capacity optimization in LTE," *IEEE Transactions on Vehicular Technology*, 2016.

[36] European Commission, *COST Action 231: Digital Mobile Radio Towards Future Generation Systems: Final Report*, European Commission, Brussels, Belgium, 1999.

[37] 3GPP TR 36.814, Technical Specification Group Radio Access Network; Evolved Universal Terrestrial Radio Access (E-UTRA); Further Advancements for E-UTRA Physical Layer Aspects, V9, March 2010.